OEA | Opto-Electronic Advances

Article

July 2026, Vol. 9, No. 7

Open Access

Unlocking home-based nocturnal health management: A fiber-optic approach for early detection of cardiorespiratory rhythm disorders

Hanyu Jin[1,4†], Hao Li[1,4,5†], Zhuolin Chen[1†], Liangye Li[3], Zurui Wang[1], Kai Zhou[1], Weijian Hang[2], Zhipeng Chen[1], Junfeng Chen[1,4], Kai Shen[4], Jianfeng Wen[4], Chen Chen[2], Cunzheng Fan[1,4], Zhijun Yan[1,4], Feng Wang[2]* and Qizhen Sun[1,4]*

Abstract: Cardiorespiratory rhythm disorders (CRD) are prevalent yet underdiagnosed conditions with substantial health risks. Current diagnostic methods are limited by invasiveness, intermittent symptom presentation, and low sensitivity during wakefulness. Sleep, by contrast, offers a stable physiological state ideal for early CRD detection. Here, we introduce a fiber-optic vital sign monitoring pillow (VSMP) that aims to realize the vision of home-based nocturnal health management, leveraging natural sleep for the accurate and unobtrusive early detection of CRD. By integrating fiber-optic sensing, biomechanical engineering, and advanced signal processing, the VSMP achieves early CRD detection through heart rate variability analysis and Lorenz scatter plots, while also facilitating blood pressure estimation (<8% error). Thus, we present VSMP as a new paradigm that transforms passive sleep into an active diagnostic session, paving the way for data-driven, personalized health management and proactive, precision medicine directly in the home environment.

Keywords: fiber-optic sensor; health monitoring; cardiorespiratory diseases; telemedicine; smart fiber; early disease screening

DOI: 10.29026/oea.2026.250334 | CSTR: 32247.14.oea.2026.250334

Citation: Jin HY, Li H, Chen ZL et al. Unlocking home-based nocturnal health management: A fiber-optic approach for early detection of cardiorespiratory rhythm disorders. *Opto-Electron Adv* **9**, 250334 (2026).

1 Introduction

Cardiorespiratory rhythm disorders (CRD), which include cardiac arrhythmias (CA) and sleep apnea (SA), represent substantial global health threats[1–6], with CA posing particularly insidious risks due to their frequently asymptomatic progression. Conditions like atrial fibrillation (AF)[7,8], sinus bradycardia (SB)[9,10] and premature beats (PB)[11–13] often advance silently in early stages, lacking overt symptoms (such as panic attacks, fainting, or dizziness) and manifesting only as transient heartbeat irregularities or subtle blood pressure changes. This clinical silence delays diagnosis, with many patients' seeking medical attention only at advanced stages when optimal treatment windows have passed. Such diagnostic delays inevitably amplify disease burden, as asymptomatic AF often remains undetected for years, markedly increasing stroke and heart failure risks. Over 60% of asymptomatic AF cases remain undiagnosed until stroke onset[7,8,14], highlighting the critical gap in early screening tools. Conventional diagnosis of CRD primarily depends on 24-hour ambulatory electrocardiography (ECG)[15] monitoring and in-laboratory polysomnography (PSG)[16]. However, these diagnostic modalities are typically accessed only after patients exhibit overt clinical symptoms, limiting their utility for early detection and timely intervention. Effective early screening for CRD therefore requires diagnostic tools

Received: 26 November 2025

Accepted: 9 March 2026

Published online: 23 April 2026

[1]School of Optical and Electronic Information, National Engineering Research Center of Next Generation Internet Access-system (NGIA), Huazhong University of Science and Technology, Wuhan 430074, China; [2]Division of Cardiology, Department of Internal Medicine and Hubei Key Laboratory of Genetics and Molecular Mechanism of Cardiologic Disorders, Tongji Hospital, Tongji Medical College, Huazhong University of Science and Technology, Wuhan 430000, China; [3]School of Information Mechanics and Sensing Engineering, Xidian University, Xi'an 710071, China; [4]HUST-Wuxi Research Institute, Wuxi 214174, China; [5]School of Electrical and Electronic Engineering, Nanyang Technological University, 50 Nanyang Avenue, Singapore 639798, Singapore.

[†]These authors contributed equally to this work.

*Correspondence: F Wang, E-mail: wangf_tjh@163.com; QZ Sun, E-mail: qzsun@hust.mail.edu.cn

that simultaneously achieve three critical attributes: high diagnostic sensitivity; user-friendly operation, and enhanced portability. These clinical requirements[14,17] highlight the urgent need for innovative home-based monitoring solutions capable of sensitive, unobtrusive longitudinal assessment-capabilities beyond the reach of current gold-standard diagnostic approaches.

While patients struggle to self-detect early-stage CRD, these disorders cause distinct alterations in core physiological parameters —heartbeat, respiration rhythm, and blood pressure. Continuous monitoring of these biomarkers enables early screening[18,19]. Conventional wearable devices often disrupt sleep and compromise compliance, leading to unreliable data. Sleep itself offers a solution: during this natural rest state, the body's minimal movement and stable physiology create ideal conditions for accurate, unobtrusive monitoring.

Current sleep monitoring devices can be broadly categorized into wearable and non-wearable technologies. Wearable devices, such as portable ECG[20–22] and photoplethysmography (PPG) devices[23–25], provide continuous monitoring by capturing cardiac electrical activity and blood volume changes, respectively. However, they require skin contact, which can be uncomfortable and disruptive to sleep quality, especially for asymptomatic individuals. Additionally, many existing wearable sensors are limited to single-parameter measurements (e.g., respiration or heartbeat[26,27]) and may not be suitable for long-term use due to skin irritation or discomfort caused by prolonged contact with rigid materials. While, non-wearable devices, such as pressure sensors embedded in mattress and radar technologies, avoid physical contact but face other limitations. In recent years, existing fiber-optic non-contact vital sign monitoring schemes[28–34] (special fiber, multimode fiber, fiber Bragg grating (FBG), etc.) only measure respiratory/heart rate and are hard to integrate into homes due to complex components. Additionally, some CA monitoring schemes combine piezoelectric film sensors[35–40], radar sensors[41–43] with artificial intelligence (AI). However, these rely on black-box machine learning models and fail to provide tangible pathogenic mechanisms, cannot serve as a reliable diagnostic tool for CA. In conclusion, this technological landscape highlights the unmet need for unobtrusive equipment combining diagnostic precision with real-world applicability.

This paper introduces an unobtrusive vital sign monitoring pillow (VSMP) that leverages a flexible fiber-optic sensor[44–46], transforming the home sleep environment into a diagnostic space. The platform wirelessly transmits data to smartphones via Bluetooth, facilitating potential integration with cloud storage for long-term health tracking and remote diagnosis. Specifically designed as a comfortable pillow, our solution eliminates the need for wearables while ensuring clinical-grade precision. Its key benefits —including seamless posture compatibility, continuous monitoring, and simple data sharing —collectively overcome the constraints of traditional techniques and establish a new paradigm for decentralized sleep medicine. The VSMP successfully captured high-quality ballistocardiography (BCG) signals from CA patients. Notably, our integrated heart rate variability (HRV)+Lomb–Scargle periodogram (LSP) analytical scheme —superior in sensitivity, specificity, and clinical applicability with explicit clinical rationale and cross-validation value—was employed to analyze the signals. These analyses enabled pathological assessment of cardiac function, demonstrating remarkable consistency with hospital ECG diagnoses, correlation index over 98% (vs. ECG data)[47,48]. The VSMP additionally identified and classified high-risk respiratory patterns associated with CA through advanced signal processing. Furthermore, an AI machine learning model was applied to achieve blood pressure prediction with <8% error by analyzing reproducible BCG segments in healthy cohorts, enabling continuous non-invasive monitoring. By transforming passive sleep into an active diagnostic window, our work thus unlocks a practical pathway to home-based nocturnal health management. It functions as a reliable auxiliary tool for early screening, effectively bridging the gap between convenient screening and clinical-grade accuracy while advancing the frontier of personalized, preventive care.

2 Method

2.1 Unobtrusive pillow sensing architecture and functions

The structure, advantages and functions of VSMP are shown in Fig. 1. When the subject lies on the pillow during sleep (Fig. 1(a)), physiological signals are continuously acquired through the embedded optical fiber sensor. The sensing fiber detects subtle pressure variations caused by cardiorespiratory activity. These mechanical signals are transmitted to the core interferometric system, which employs phase demodulation technology to convert them into quantifiable physiological data. The reference-fiber and other components are encapsulated together in an enclosure, as shown in Fig. 1(a-i). The sensing fiber is encapsulated within a multilayer composite of viscoelastic organic materials, (Fig. 1(a-ii)) achieving dual functionality: enhanced axial strain sensitivity for 115× through optimized material modulus matching; and effective attenuation mechanical noise transmission from the bed substrate via impedance mismatch principles (specific functional characteristics are detailed in the Section *Methods*). Three PIN detectors transmit the received interference signals via Bluetooth to mobile devices. The devices then perform optical phase signal demodulation to obtain the vital signal (Fig. 1(a-iii)).

Figure 1(b) demonstrates the sensing principle and key functionalities of the VSMP. Pressure variations at the human carotid artery are transmitted through the pillow and sensitization structure to the sensing optical fiber, inducing

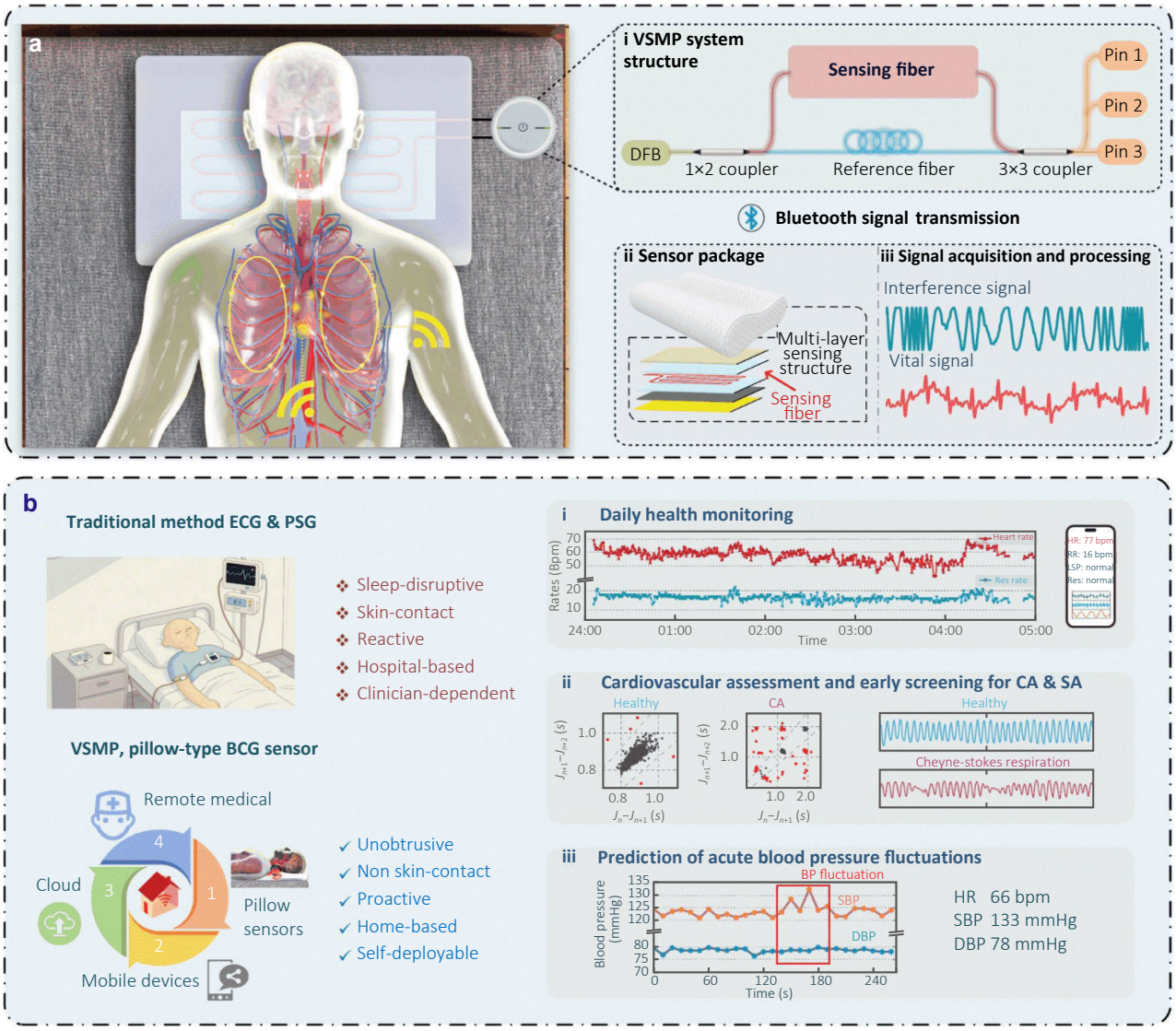


Fig. 1 | VSMP architecture, advantages and functions. (a) VSMP system structure and data flow diagram. i, VSMP optical path structure. ii, the structure of the pillow-type sensor and the multi-layer encapsulation sensitisation structure of the sensing optical fiber. iii, interference alternating current signals collected by the VSMP and raw physiological signals obtained by terminal demodulation. (b) 5 major advantages of VSMP compared to traditional monitoring solutions (unobtrusive, non skin-contact, proactive, home-based and self-deployable) and remote healthcare workflow of the VSMP. Three main application functions: i, daily health monitoring; ii, cardiovascular assessment and early screening for CA & SA; iii, prediction of acute blood pressure fluctuations.

phase shifts in the optical signal (detailed principles and design in Supplementary Section 1). In contrast to traditional SA and CA detection approaches, VSMP offers five distinct advantages: unobtrusive, non skin-contact, proactive, home-based and self-deployable. The VSMP's all-single-mode-fiber sensor architecture enables seamless integration with residential Fiber-to-the-Room (FTTR) infrastructure; crucially, the system allows for multi-user signal acquisition with a single terminal simply by adding extra couplers and detectors. This unique scalability positions the VSMP as a critical physiological monitoring node in remote medical diagnosis, bridging domiciliary and clinical domains. Embedded fiber-optic sensors unobtrusively acquire BCG and respiratory signals during sleep, which are wirelessly transmitted to mobile devices for real-time preliminary analysis of CRD. Processed datasets are subsequently synchronized to secure cloud platforms for longitudinal analysis and clinical data management, enabling remote healthcare providers to deliver personalized diagnostic feedback and preventive recommendations through the connected telehealth interface.

The VSMP platform integrates three key functional modules to enable comprehensive nocturnal monitoring: continuous physiological surveillance (nocturnal respiration, beat-to-beat heart rate, and body movement); multimodal cardiovascular analytics (LSP and HRV for CA/SA

detection); and blood pressure prediction for tracking nighttime fluctuations. To our knowledge, this represents the first demonstration of an unobtrusive platform capable of acquiring diagnostically meaningful BCG signal from CA patients without skin contact even amid the challenges posed by complex cardiac mechanics[38,39]. These signals exhibit high consistency with the gold standard ECG signal and are suitable for pathological analysis using LSP and HRV techniques. Notably, the extracted BCG waveforms exhibit strong temporal and morphological correlation with ECG, validating the system's ability to provide clinically relevant cardiovascular data through a fully unobtrusive approach.

2.2 VSMP sensor unit structure

In the VSMP, all components except the pillow-embedded sensing fiber are enclosed in an integrated box. A multi-dimensional organic material wrapping (Fig. 1(b-ii)) replaces lossy traditional mesh structures to address the fiber's inherent axial stress insensitivity, achieving 115× sensitivity improvement (details in Supplementary information of Sections 3-4) via noise isolation and weak signal enhancement. This layered structure amplifies target signals while suppressing noise, effectively lifting the system's detection limit and endowing the VSMP with strong weak signal detection capability. The VSMP uses a 3×3 Mach-Zehnder interferometer (MZI) interferometer for phase demodulation, outputting three 120° phase-shifted interference signals for direct, accurate demodulation via a simple algorithm. Combined with the fiber's multi-layer encapsulation and sensitization, this further enhances sensitivity and lifts the detection limit for weak signals, ultimately realizing reliable CRD signal detection in patients.

2.3 VSMP data pre-processing and BCG-based monitoring principles

The VSMP relies on high-fidelity BCG signals for accurate cardiovascular assessment and CA diagnosis, making signal restoration a critical first step. As illustrated in Fig. 2(a), the VSMP preprocessing pipeline begins with optical interference signal acquisition through the terminal box's analog-to-digital converter (ADC) module, which transmits raw data to the host device for processing. The host device performs phase demodulation to extract vital signs encompassing respiratory, cardiac, and body movement components. Subsequent processing involves filtering out segments contaminated by body movements. Notably, while respiratory signals remain stable, BCG signal quality can be significantly compromised in certain side-lying positions, fortunately, humans typically spend sufficient time in the supine position during sleep, ensuring an adequate window for data collection. The VSMP selectively processes segments where the tester maintains a supine position. The final stage applies specialized filtering to these supine resting segments to yield optimized, high-fidelity BCG signals suitable for clinical analysis. The detailed pre-processing procedure is outlined in Supplementary Section 4.

The study cohort comprised healthy volunteers (faculty and students from Huazhong University of Science and Technology) and cardiology participants (patients recruited from the cardiology ward of the Tongji Hospital of China). The CA-suspected inpatients requiring continuous ECG

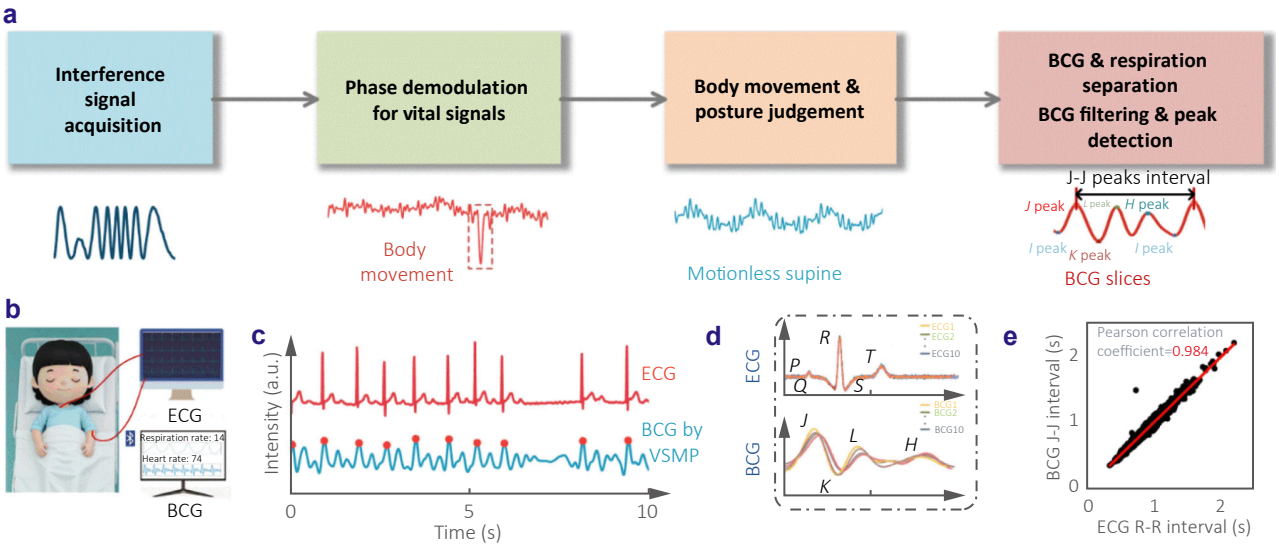


Fig. 2 | VSMP data pre-processing and BCG-based monitoring principles. (a) The VSMP signal preprocessing workflow includes signal acquisition, phase demodulation, body movement and sleeping position screening, and filtering separation processes. (b) Schematic of a patient undergoing simultaneous ECG and VSMP monitoring. (c) The BCG signals obtained by VSMP and the ECG signals form effectively contrasting resultant fragments. (d) Comparison of standard ECG and BCG signals. (e) Correlation analysis and fitting results of BCG J-J peak and ECG R-R peak heart rate intervals.

monitoring during their first hospitalization day were enrolled with informed consent. ECG data were collected from a subset of these patients, and some underwent concurrent VSMP and ECG monitoring on the same day, as illustrated in Fig. 2(b). Figure 2(c) presents a comparison between the ECG signals obtained using a commercial device and the BCG signals acquired by the VSMP for one patient. Figure 2(d) compares standard ECG and BCG waveforms. The correlation coefficient of the heart rate intervals extracted from the ECG and BCG signals reached 0.984, which suggests that BCG signals can be subjected to analytical approaches similar to those used for ECG signal processing, also shown in Fig. 2(e). This high ECG correlation verifies the reliability of the VSMP for heart rate interval monitoring, positioning the device as a home-based auxiliary tool for early warning of cardiac abnormalities. Figure S2 shows more sample fragments corresponding to BCG and ECG.

2.4 Volunteer information & declaration of human subject study

During the data collection phase, we recruited 20 CRD patients and over 60 healthy subjects. All 20 CRD patients had their conditions successfully detected by the VSMP system. These 20 CRD patients were categorized into four clinical subtypes by pathological features, with one representative case per subtype selected for in-depth analysis in the main text. Table S4 in the supplementary materials provides full details of all 20 CRD patients, including non-representative cases beyond the 4 typical samples. Figure S11 presents partial LSP diagnostic results for the testers not elaborated on in the main text. Additionally, 5 age- and gender-matched healthy volunteers were recruited as controls. This study focuses on comparative analysis of these 9 representative subjects. Their demographic details are presented in Tables S2 and S3. All CRD patients were recruited from Tongji Hospital's Cardiology Department. Written informed consent was obtained from all participants per relevant guidelines. Partial on-site data collection processes are shown in Fig. S6.

3 Results and discussion

3.1 VSMP daily health management

The VSMP provides comprehensive, daily nocturnal health monitoring by tracking key vital signs such as sleep respiratory rate and heart rate, while also detecting bed exits and body movements[47,48]. In this study, we employ HRV, LSP, and related analytical methods to further validate its capability for early cardiovascular risk assessment and ongoing health management. LSP provides an intuitive assessment of whether a user is experiencing cardiac arrhythmia, with HRV serving as a supplementary indicator to better observe the test subject's long-term cardiac condition.

This study utilised time-domain HRV indices to analyse the cardiac health status of test subjects, including: SDNN, RMSSD, pNN50, pNN30, and PV15, the interpretation of these indicators[49] and what they represent is described in detail in the Table S1, each parameter is calculated by filtering signals over a fixed period of time.

Younger individuals generally have stronger autonomic regulation and more active vagal function, enabling rapid heart rate adjustments to meet physiological demands, resulting in higher SDNN and RMSSD values. In contrast, these values decrease with age. Additionally, within the same age group, gender differences are observed: males tend to have higher SDNN values, while females have higher RMSSD values. Figure 3(a) and 3(b) present the long-term SDNN and RMSSD average results and burden ranges for $V_{1\text{-}5}$, demonstrating a clear age-related decline and confirming the HRV results obtained from VSMP monitoring are consistent with the characteristic distribution of age and sex[49,50].

To further elucidate the variations of these indicators across distinct physiological states, the VSMP was employed for continuous monitoring of V_1. Figure 3(c) illustrates the HRV metrics obtained from VSMP monitoring of V_1 under four distinct conditions: normal resting, post all-night, post-alcohol consumption, and post-strenuous exercise.

Theoretically, staying up all night is expected to inhibit autonomic nervous system regulation and parasympathetic nerve activity, leading to decreased HRV. Similarly, alcohol consumption is known to suppress parasympathetic activity while increasing sympathetic excitability, resulting in elevated heart rate and reduced HRV. After an all-night vigil, S_1 exhibited a 5% decrease in average NN interval (AVNN), a 13% decrease in SDNN, and a 35% decrease in RMSSD compared to the normal condition, with no significant changes in pNN50 and pNN30. In contrast, following alcohol consumption, AVNN decreased by 13%, SDNN by 66%, RMSSD by 62%, and both pNN50 and pNN30 decreased substantially by 60% and 83%, respectively. These results highlight the significant impact of alcohol consumption on both the autonomic and parasympathetic nervous systems[51].

Acute exercise is theorized to increase heart rate through sympathetic activation, which is necessary to meet the elevated oxygen and energy demands during physical activity. This sympathetic arousal is also expected to suppress autonomic regulation, leading to a decrease in HRV[52]. Compared to the normal condition, after a short period of strenuous exercise, V_1 experienced a 24% reduction in AVNN, a 64% reduction in SDNN, a 62% reduction in RMSSD, and significant reductions of 63% and 81% in pNN50 and pNN30, respectively.

Beyond monitoring stable health parameters in normal subjects, VSMP has successfully extended its capabilities to diverse populations with varying health conditions, yielding clinically meaningful results. Figure 3(d–f) present the BCG

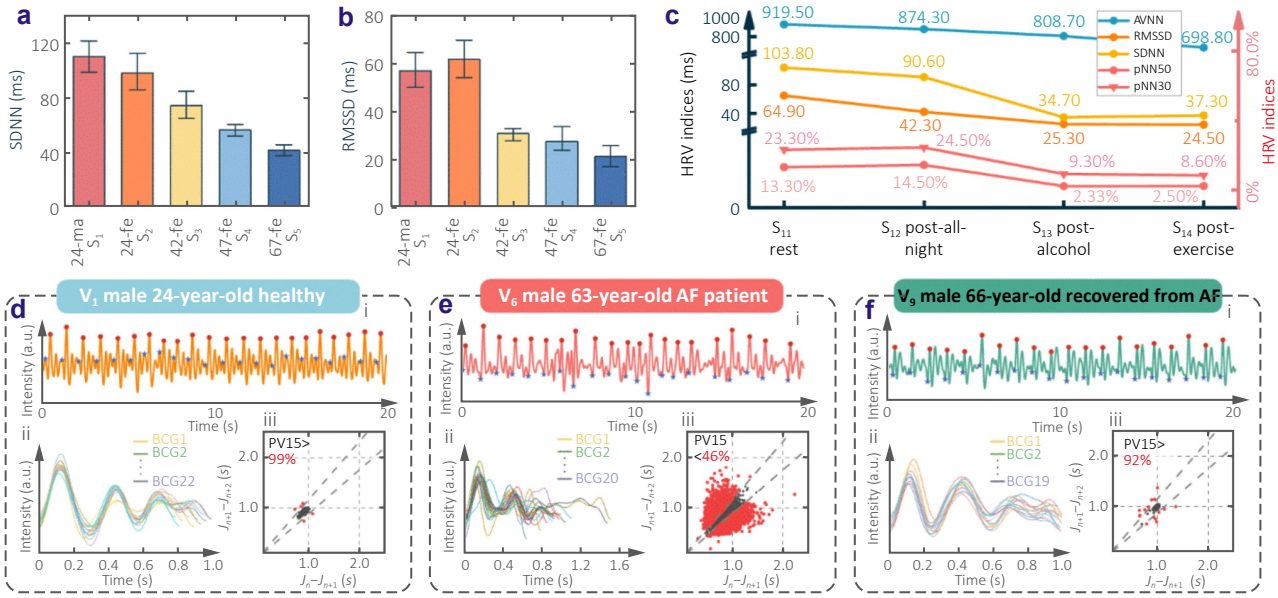


Fig. 3 | HRV index data in S_1–S_5 and results of BCG sections and analyses. Mean values and range of variation for SDNN (a) /RMSSD (b) under continuous monitoring of $V_{1–5}$. (c) Variation of HRV indicators in different scenarios for V_1. (d) BCG sections LSP results of V_1. (e) BCG sections and LSP results of V_6. (f) BCG sections and LSP results of V_9.

signal fragments, individual BCG slices, and LSP results with their corresponding PV15 indices for three volunteers: V_1, 24-year-old healthy male; V_6, 63-year-old patient with AF, and V_9, 66-year-old patient with recovered AF, over a 30-minute monitoring period. The result of V_1 (Fig. 3(d)) showed highly repeatable BCG signals, stable waveforms, strongly aggregated LSP results, and a PV15 index exceeding 99%. In contrast, the AF patient (Fig. 3(e)) exhibited highly variable waveforms, poor repeatability, and dispersed LSP results with no clear aggregation, with a PV15 index below 46%, reflecting the irregular heartbeat caused by AF[53]. The patient who had undergone cox-maze surgery (Fig. 3(f)) demonstrated improved BCG waveform repeatability and a PV15 index above 88%.

These results confirm that the VSMP holds promise for widespread adoption in daily health monitoring, as it provides robust assessments for individuals with varying health statuses, underscoring its broad applicability.

3.2 Cardiovascular assessment and detection of CRD

Patients with CA-like diseases often exhibit highly disordered cardiac rhythms, primarily due to abnormal electrical activity in the atria. This disorder results in a complete loss of aggregation in their LSP results[54,55]. Therefore, the directly calculated HRV indices for these patients show a marked increase.

Figure 4 presents a selection of data results obtained via VSMP during continuous monitoring of patients with various CA (volunteers 6–9). Figure 4(a) and 4(b) respectively display the range of variation and mean values of SDNN and RMSSD data calculated by VSMP for these samples. The red horizontal lines in these figures denote the reference results derived from ECG data (owing to hospital regulations, ECG signals could only be collected from patients prior to surgery for one day).

V_6 is a typical patient with persistent AF, and the corresponding BCG segments and LSP results from S6 were previously shown in Fig. 3(b). As depicted in Fig. 4(a) and 4(b), the mean values of SDNN and RMSSD for this patient were 221 ms and 300 ms, respectively. The reference ECG data obtained on the same day were 212 ms and 293 ms, with discrepancies of less than 5%. Figure 4(c) and 4(d) show continuous comparison graphs of six HRV indices calculated by VSMP and the reference ECG data for four time periods during the test night. The VSMP results closely match the ECG data.

V_7 is a patient with paroxysmal AF and premature beats (PB), was tested on the day before and the day after AF ablation surgery (Cox-Maze surgery), respectively. As shown in Fig. 4(a) and 4(b), before the surgery, the patient's mean SDNN and RMSSD values were 127 ms (range: 118–142 ms) and 226 ms (range: 208–251 ms), respectively. The preoperative ECG data yielded mean values of 112 ms and 202 ms. Although the ECG and BCG data were not collected on the same day, introducing some bias, the VSMP data still effectively captured the patient's abnormal conditions.

BCG slices extracted from $S_{7,p}$ and $S_{7,a}$ are shown in Fig. 4(e) and 4(f). Before the surgery, two distinct BCG lengths were primarily observed in the patient's BCG slices: 0.5 s and 1 s, respectively, in a roughly 1∶2 relationship. This indicates the presence of PB and intermittent atrial flutter with a

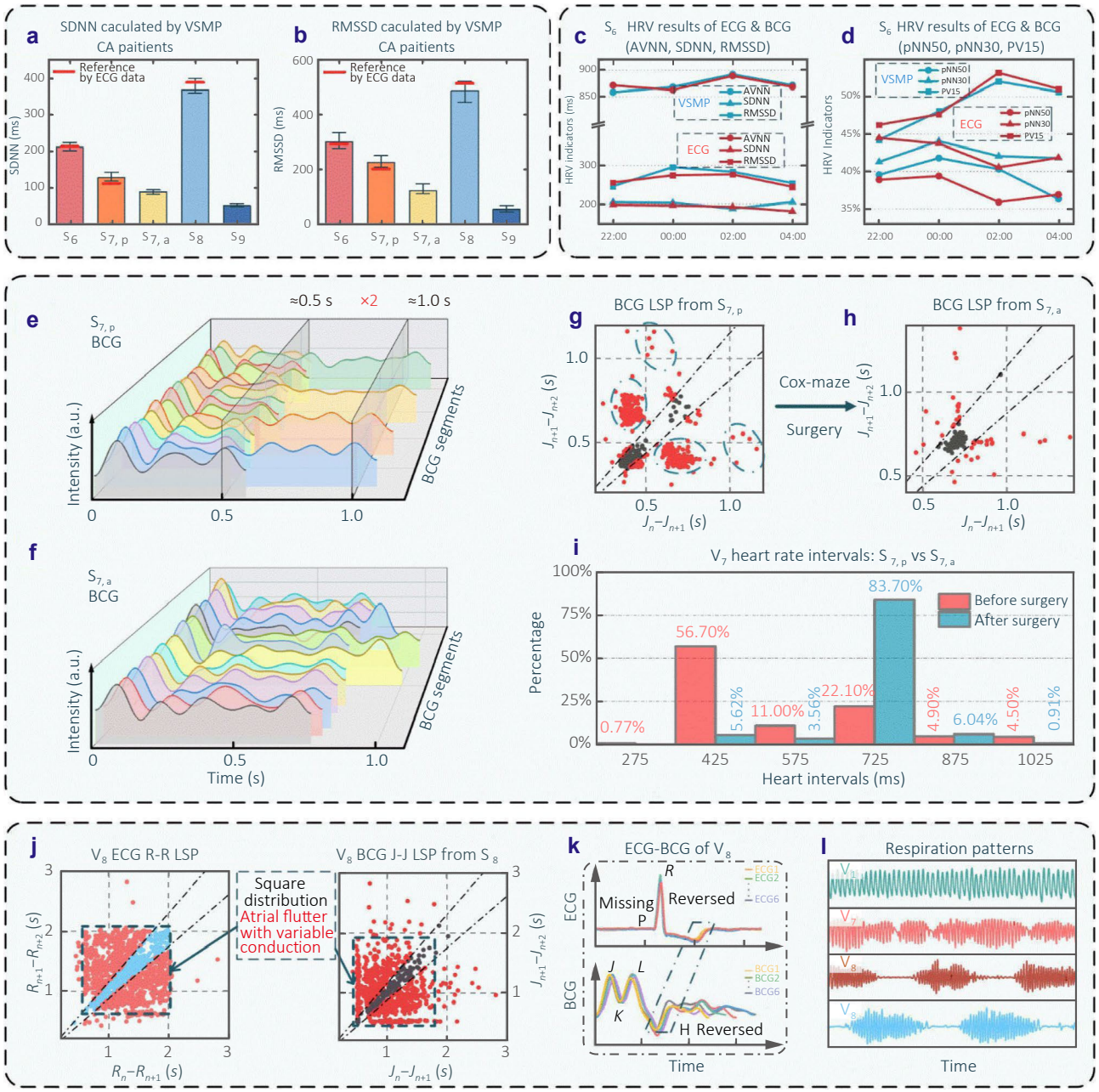


Fig. 4 | Cardiovascular assessment and detection of CA & SA. Mean values and range of variation for SDNN (a) /RMSSD (b) under continuous monitoring of $S_{6\text{-}9}$. (c) Comparison of HRV indices (SDNN, AVNN, RMSSD) calculated for S_6, from VSMP and ECG. (d) Comparison of HRV indices (pNN50, pNN30, PV15) calculated for S_6, from VSMP and ECG. (e) BCG segments of V_7 before surgery. (f) BCG segments V_7 after surgery. (g) LSP result of V_7 before surgery. (h) LSP result of V_7 after surgery. (i) Statistical distribution of heart rate intervals before and after surgery performed on V_7. (j) Comparison of LSP results of V_8 calculated by ECG and by VSMP data (not the same day). (k) Comparison of waveforms of abnormal BCG signal and abnormal ECG signal of V_8, it can be seen that the T-peak of ECG and BCG H-peak are inverted. (l) Comparison of normal vs. abnormal respiratory signals acquired by VSMP (250 s signal segment).

2∶1 conduction ratio[56,57], leading to frequent occurrences of heart rate intervals in a 2:1 relationship. Figure 4(g) presents the LSP result of $S_{7,p}$, revealing four distinct clusters of LSP results, all within the regions of heart rate intervals of 2∶1 and 1∶2. The LSPs obtained from ECG calculations also show the same distribution (as shown in Fig. S4).

After surgery, the patient's SDNN and RMSSD indices decreased to 88 ms (range: 82–94 ms) and 128 ms (range: 111–147 ms), respectively. Figure 4(f) shows that most heart rate results in the BCG slices have returned to normal, though some BCG lengths are still longer than usual. Figure 4(h) displays the $S_{7,a}$ LSP results, indicating that heart rate

intervals have largely normalized to a ±15% variation range. Figure 4(i) illustrates the statistical distribution of J-J intervals obtained from $S_{7,p}$ and $S_{7,a}$, highlighting a more aggregated distribution after surgery. Some abnormal results in the RMSSD data and LSP results after surgery may be attributed to the fact that the data were collected on the night following the surgery, when the heart was still in an incomplete state of recovery. In contrast, S9, whose data were collected three days after surgery, shows that the patient's indices have essentially returned to normal, as depicted in Fig. 4(a) and 4(b).

V_8 is a patient with AF and cardiac hypertrophy. S8 exhibited very exaggerated abnormalities in SDNN and RMSSD, with values as high as 368 ms (range: 333–400 ms) and 489 ms (range: 445–523 ms), respectively. The corresponding metrics computed from the patient's ECG were 389 ms and 513 ms, respectively (note that the ECG and BCG data were not collected on the same day). Both parameters were abnormally elevated, indicating more than just a rhythmic abnormality associated with AF. Figure 4(j) displays the LSP results derived from both ECG and BCG, both of which exhibited a clear square distribution.

Given that the V8 suffers from severe cardiac hypertrophy, this condition may result in altered electrophysiological properties of the atria and ventricles, thereby affecting atrioventricular conduction. The hypertrophied myocardium may increase the electrical conduction resistance of the myocardium, leading to delayed or irregular atrioventricular conduction. Moreover, cardiac hypertrophy may induce structural and functional changes in the atria, increasing the risk of atrial flutter and resulting in instability in the atrioventricular conduction ratio and unequal downward transmission of atrial flutter[58,59] (atrial flutter with variable conduction).

V_8's complex cardiac problems are not only reflected in rhythmic abnormalities on the ECG. The usual ECG signals of such patients with AF are missing the P-wave, but as shown in Fig. 4(k), the ECG signal of V_8 is not only missing the P-wave compared to the normal signal, but also shows the phenomenon of T-wave inversion. This is due to cardiomyocyte hypertrophy and increased oxygen consumption in cardiac hypertrophy, which may lead to myocardial repolarization abnormalities, and consequently, T-wave hypoplasia or inversion. In the BCG signal of S8, as shown in Fig. 4(k), the same phenomenon of H-wave inversion in the waveform was observed, which may reveal a certain degree of correspondence between the T-wave in the ECG signal and the H-wave in the BCG signal. Cardiac patients demonstrate heightened susceptibility to respiratory comorbidities. The VSMP trials revealed a graded association between the severity of CA and the prevalence of concomitant respiratory disorders. Figure 4(l) presents representative respiratory waveforms from different volunteer cases: V_1 (health) demonstrates stable respiratory amplitude and rhythm, serving as the normative reference; V_7 (AF with PB) exhibits characteristic Cheyne-Stokes respiration patterns with periodic amplitude modulation and transient apnea episodes (3–5 s duration). The final two waveforms originated from V_8, a case exhibiting cardiomegaly (3× normal volume), atrial flutter with variable conduction. The marked cardiac enlargement caused significant pulmonary compression, exacerbating respiratory dysfunction. These recordings reveal severe sleep apnea featuring 90-second cyclic patterns: 60 seconds of Cheyne-Stokes respiration followed by 30 seconds of apnea clinically critical respiratory rhythm.

Overall, the VSMP's efficacy in monitoring volunteers with CRD positions it as a catalyst for a proactive prevention paradigm. By reliably detecting conditions ranging from early paroxysmal AF to severe persistent AF via the integrated HRV-LSP diagnostic approach, the system enables a seamless continuum from early discovery to ongoing management, which is fundamental to effective personal health management strategies.

3.3 AI powered continuous blood pressure monitoring

Notably, early-stage CRD can induce subtle yet clinically significant blood pressure fluctuations, underscoring the importance of integrated hemodynamic monitoring for comprehensive risk assessment. Owing to the challenges in acquiring reliable real-time blood pressure data from subjects within the hospital environment, a preliminary assessment of the VSMP's blood pressure monitoring capability was performed in a controlled laboratory setting with three volunteers. Since BCG waveforms are known to reflect cardiovascular dynamics, we leveraged the high-fidelity BCG signals captured by the VSMP to develop a blood pressure prediction model. The system's ability to consistently extract stable BCG waveforms under real-world conditions lays a solid foundation for continuous BP tracking. This capability is supported by our previous transfer attempts of mature, well-validated BP prediction models[60–62] that rely on pulse wave waveforms, which enables the system to serve as a practical tool for daily health management. This functionality not only enhances early disease detection but also supports long-term monitoring, aligning with the goal of proactive home-based health management. A cuff sphygmomanometer was used as the reference device, with 120 blood pressure measurements collected per condition from three subjects as training data. Figure 5(a) illustrates the experimental setup, while Fig. 5(b) depicts a representative BCG signal with annotated peaks. The temporal intervals and slopes between these peaks were extracted as features for machine learning (Fig. 5(c)). Correlation analysis in Fig. 5(d) and 5(e) reveals that multiple features exhibit strong correlations ($|r| > 0.7$) with both systolic and diastolic blood pressure, supporting their utility in prediction.

To verify the VSMP's ability to monitor a larger dynamic range of blood pressure, V_1 and V_2 were selected for

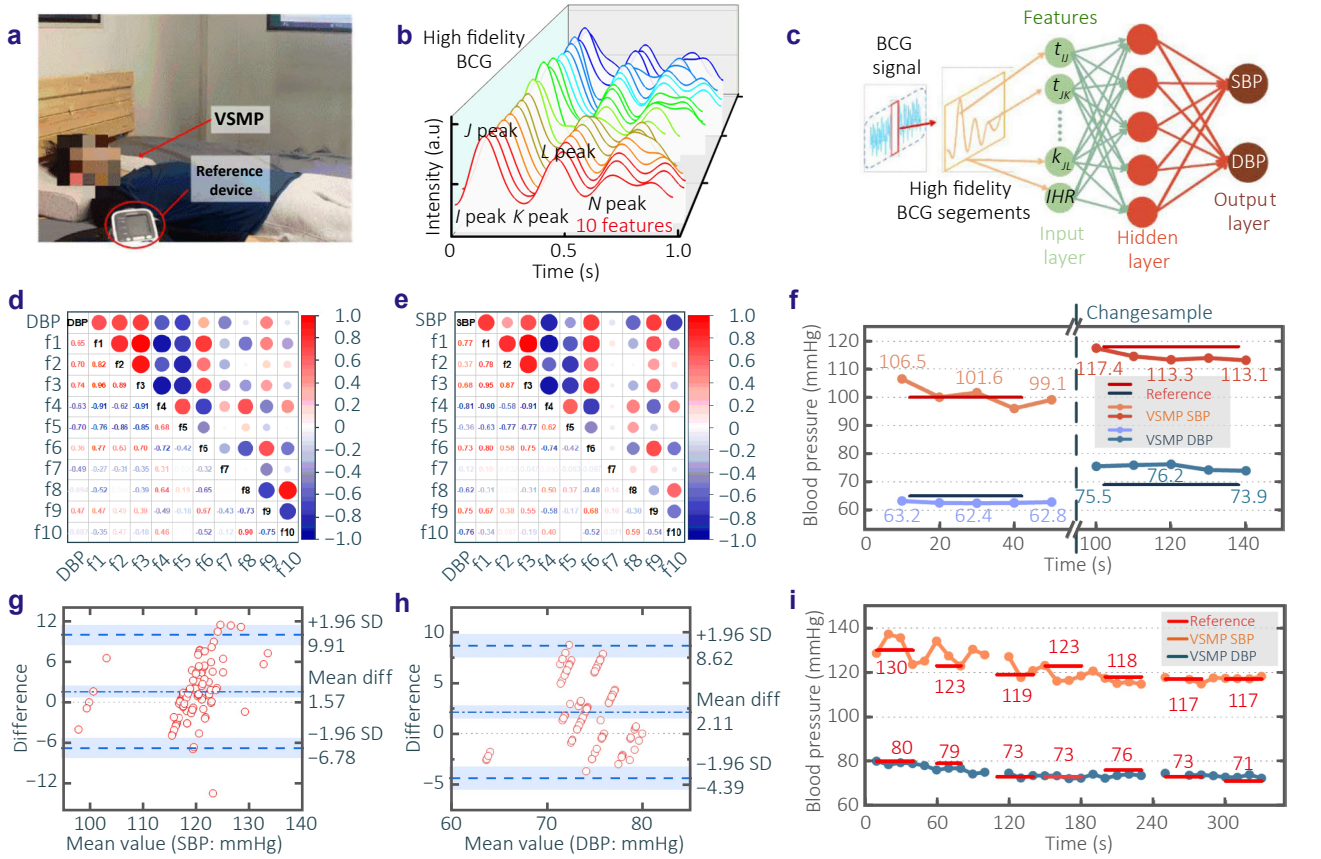


Fig. 5 | Results of blood pressure monitoring at VSMP. (a) Schematic diagram of VSMP blood pressure monitoring and reference data sources. (b) BCG signal slices and peak infographics. (c) Machine learning model for extracting feature values from BCG for blood pressure calculation. (d) Pearson correlation plots for DBP and 10 eigenvalues. (e) Pearson correlation plots for SBP and 10 eigenvalues. (f) Blood pressure values obtained from VSMP calculations by changing testers (volunteer 2 to 1, S_2 to S_{15}) during continuous blood pressure monitoring. (g) Bland-Altman error analysis of SBP calculation results. (h) Bland-Altman error analysis of DBP calculation results. (i) Blood pressure monitoring results by VSMP after strenuous exercise (V_1, S_{14}).

dynamic blood pressure testing, both of which exhibited significant variations in baseline blood pressure. The testing process is recorded in Supplementary Movie 1. During the test, V_2 was tested first, and four sets of blood pressure values were obtained after 40–50 s of testing (cuff sphygmomanometer testing typically takes 30–50 s). As shown in Fig. 5(f), the VSMP successfully demonstrated continuous blood pressure monitoring across both test samples, confirming its wide dynamic range capability. (Fig. S5 shows comparisons of BCG slices from the same sample with the same heart rate but different blood pressures, and other BCG comparisons for similar conditions.)

Subsequently, we performed blood pressure on the three testers using the trained model. Bland-Altman error analysis plots (Fig. 5(g) and 5(h)) show errors within −6.78 to 9.91 mmHg for SBP and −4.39 to 8.62 mmHg for DBP, all within an 8% margin.

Sudden strenuous exercise is known to elevate blood pressure quickly[63,64]. To test the VSMP's responsiveness, V1 performed ten minutes of strenuous exercise, followed by continuous blood pressure monitoring with VSMP. The results are shown in Fig. 5(i) (with the test procedure in supplementary movie material 2). Notably, around the six-minute mark, V_1's blood pressure began to gradually decrease, which was accurately captured by the VSMP.

Integral to the paradigm of proactive home-based health management, the VSMP's blood pressure prediction capability shows potential for the early identification of nocturnal cardiovascular instability associated with CRD episodic sleep into an ongoing opportunity for risk monitoring and personalized health management. This approach underscores the system's considerable application prospects in home-based cardiovascular health monitoring.

3.4 Discussion

The VSMP, a home-based CRD early screening tool, features notable multi-disciplinary integration, combining optical engineering, clinical medicine, and information science to translate fiber-optic sensing signals into clinically interpretable indicators. This addresses the critical need for early CRD screening, as intermittent, asymptomatic early-

stage disorders are often missed by traditional hospital monitoring. Specifically designed for domestic settings, future work will continue to rely on machine learning models to perform sample recognition by analysing the time-frequency domain characteristics of different sample signals, enabling tailored monitoring for multiple family members. Beyond CRD screening, the VSMP caters to healthy test subjects by enabling long-term HRV monitoring, which assesses the capacity for active heart rate regulation and holds significant importance for the early screening of certain diseases. Overall, the VSMP enables unobtrusive home monitoring for diverse populations, facilitating timely intervention and reducing healthcare burdens.

Future optimization of the VSMP will focus on three key directions to further elevate its performance and clinical utility. First, developing posture-adaptive denoising algorithms, optimizing pillow sensor configurations for side-lying body positions, and leveraging AI-driven data migration strategies to process anomalous BCG signal data effectively. Second, we will expand the sample scale for blood pressure prediction models and CRD patient cohorts, implement long-term individual monitoring protocols, and refine model accuracy via transfer learning techniques. Third, advancing the integration with FTTR infrastructure and deepening telemedicine collaborations to consolidate CRD monitoring capabilities and enhance the cross-scenario clinical translational value of the system.

4 Conclusions

In this paper, we present an unobtrusive sleep-monitoring pillow, offering a radiation-free platform for continuous physiological tracking. The VSMP leverages an ultra-sensitive fiber-optic sensor to capture high-fidelity BCG signals from the carotid artery region, achieving the first reported contact-free unobtrusive monitoring of diagnostically meaningful BCG waveforms in CA patients, waveforms highly consistent with gold-standard ECG and suitable for LSP/HRV-based pathological analysis. In CA patients, the system demonstrated strong agreement with ECG in heart rate intervals (correlation: 0.984) and HRV parameters (SDNN, RMSSD errors <5%), enabling accurate pathological diagnosis via HRV and LSP analysis consistent with clinical etiology. The platform also identified high-risk respiratory symptoms linked to CA, showing particular utility in early screening for paroxysmal cases. Meanwhile, by extracting temporal and morphological features from stable BCG segments, the VSMP achieved continuous blood pressure estimation with errors within 8% of cuff-based measurements, successfully tracking dynamic BP changes during small-scale laboratory testing. In summary, our fiber-optic VSMP exemplifies the transformative potential of interdisciplinary convergence, combining breakthroughs in fiber-optic sensing, biomechanical engineering, and advanced signal processing to unlock a practical pathway to home-based nocturnal health management. Functioning as a reliable clinical auxiliary tool to detect hidden cardiac issues early via convenient at-home monitoring and deliver timely warnings, this fiber-optic approach effectively bridges the gap between home-based convenience and clinical-grade insight, advancing a new paradigm of proactive, personalized health management.

References

1. Javaheri S, Barbe F, Campos-Rodriguez F et al. Sleep apnea: types, mechanisms, and clinical cardiovascular consequences. *J Am Coll Cardiol* **69**, 841–858 (2017).
2. McDermott M, Brown DL. Sleep apnea and stroke. *Curr Opin Neurol* **33**, 4–9 (2020).
3. Mehra R. Sleep apnea and the heart. *Cleve Clin J Med* **86**, 10–18 (2019).
4. Ali H, Lupo P, De Ambroggi G et al. Supraventricular arrhythmia with discordant electrocardiographic features: what is the arrhythmia mechanism. *Ann Noninvasive Electrocardiol* **24**, e12595 (2019).
5. Berik Safçi S. The prevalence and polysomnographic characteristics of treatment-emergent central sleep apnea with obstructive sleep apnea. *Sleep Breath* **28**, 1245–1250 (2024).
6. Diallo I, Pak VM. Metabolomics, sleepiness, and sleep duration in sleep apnea. *Sleep Breath* **24**, 1327–1332 (2020).
7. Kirchhof P, Sanders P. My atrial fibrillation is not your atrial fibrillation. *Eur Heart J* **38**, 2608–2611 (2017).
8. Dewar RI, Lip GYH. Identification, diagnosis and assessment of atrial fibrillation. *Heart* **93**, 25–28 (2007).
9. Colvert J, Greenough G. Central sleep apnea and sinus bradycardia. *Sleep* **44**, A322 (2021).
10. Khandelwal K, Madathala RR, Chennaiahgari N et al. Steroid-induced sinus bradycardia. *Cureus* **13**, e15065 (2021).
11. Zhang XY, Li JQ, Cai ZP et al. Premature beats rejection strategy on paroxysmal atrial fibrillation detection. *Front Physiol* **13**, 890139 (2022).
12. Ghosh A, Sriram CS, Pandurangi UM. A mature analysis of premature beats. *Pacing Clin Electrophysiol* **46**, 1212–1214 (2023).
13. Wu D, Xia XJ. Frontiers in premature beats research: a bibliometric analysis. *Front Cardiovasc Med* **11**, 1343274 (2024).
14. Katsanos AH, Kamel H, Healey JS et al. Stroke prevention in atrial fibrillation: looking forward. *Circulation* **142**, 2371–2388 (2020).
15. Economou Lundeberg J, Engstrom G, Dziubinski M et al. A prediction model for ventricular tachycardia events using 24h ambulatory ECG. *Eur Heart J* **43**, ehac544.405 (2022).
16. Wang JQ, Zhao S, Zhou YX et al. Narcolepsy diagnosis with sleep stage features using PSG recordings. *IEEE Trans Neural Syst Rehabil Eng* **31**, 3619–3629 (2023).
17. Srinivas S, Vignesh RKB, Ayinapudi VN et al. Neurological consequences of cardiac arrhythmias: relationship between stroke, cognitive decline, and heart rhythm disorders. *Cureus* **16**, e57159 (2024).
18. Chee K, Coles D, McGill D. Is P wave duration on 12-leads ECG useful to select ischemic stroke patients for 24h ambulatory Holter monitoring. *Heart, Lung Circ* **19**, S220 (2010).
19. Moula AI, Parrini I, Tetta C et al. Obstructive sleep apnea and atrial fibrillation. *J Clin Med* **11**, 1242 (2022).
20. Ramasamy S, Balan A. Wearable sensors for ECG measurement: a review. *Sens Rev* **38**, 412–419 (2018).
21. Wang N, Zhou J, Dai GH et al. Energy-efficient intelligent ECG monitoring for wearable devices. *IEEE Trans Biomed Circuits Syst* **13**, 1112–1121 (2019).
22. Wang JQ, Fujiwara T, Kato T et al. Wearable ECG based on impulse-radio-type human body communication. *IEEE Trans Biomed*

Eng **63**, 1887–1894 (2016).
23. Davies HJ, Bachtiger P, Williams I et al. Wearable in-ear PPG: detailed respiratory variations enable classification of COPD. *IEEE Trans Biomed Eng* **69**, 2390–2400 (2022).
24. Lapsa D, Janeliukstis R, Metshein M et al. PPG and bioimpedance-based wearable applications in heart rate monitoring-a comprehensive review. *Appl Sci* **14**, 7451 (2024).
25. Zhou XY, Pan JQ, Zhang ZN et al. Gesture-related two-factor authentication for wearable devices via PPG sensors. *IEEE Sens J* **23**, 13114–13126 (2023).
26. Chen L, Wang YH, Wen YL et al. Organic photoplethysmography sensors for wearable health monitoring. *Laser Photon Rev* **19**, 2401992 (2025).
27. Seo SW, Egharevba N. Tapered fiber optic sensor for arterial pulse wave monitoring. *Opt Fiber Technol* **87**, 103929 (2024).
28. Tan FZ, Chen SY, Lyu WM et al. Non-invasive human vital signs monitoring based on twin-core optical fiber sensors. *Biomed Opt Express* **10**, 5940–5951 (2019).
29. Lyu WM, Chen SY, Liu ZY et al. Non-invasive vital signs monitoring and premature beats recognition system based on a six holes high birefringence fiber. In *Proceedings of the 28th International Conference on Optical Fiber Sensors* W4.51 (Optica Publishing Group, 2023). https://doi.org/10.1364/OFS.2023.W4.51.
30. Chen WJ, Zhang Y, Yang HC et al. Non-invasive measurement of vital signs based on seven-core fiber interferometer. *IEEE Sens J* **21**, 10703–10710 (2021).
31. Zou CK, Wang Z, Xiao K et al. Plastic optical fiber with spherical lens embedded in mattress for sleep monitoring. *IEEE Sens J* **25**, 17144–17152 (2025).
32. Chen SY, Huang ZY, Tan FZ et al. Vital signs monitoring using few-mode fiber-based sensors. *Proc SPIE* **10814**, 108140P (2018).
33. Wang Q, Lyu WM, Chen SY et al. Noninvasive human ballistocardiography assessment based on deep learning. *IEEE Sens J* **23**, 13702–13710 (2023).
34. Li YH, Chen Y, Liu HL et al. Respiration and heartbeat signal acquisition method based on fiber optic sensing. *Chin J Lasers* **49**, 0406004 (2022).
35. Jiao X, Wang XS, Wang XH et al. Noncontact sleep monitoring system under a mattress. *IEEE Access* **9**, 111203–111213 (2021).
36. He J, Li S, Hou XJ et al. A non-contact flexible pyroelectric sensor for wireless physiological monitoring system. *Sci China Inf Sci* **65**, 122402 (2022).
37. Cinotti E, Centracchio J, Parlato S et al. A narrowband IoT personal sensor for long-term heart rate monitoring and atrial fibrillation detection. *Sensors* **24**, 4432 (2024).
38. Su QS, Huang YQ, Wu XM et al. Atrial fibrillation detection based on a residual CNN using BCG signals. *Electronics* **11**, 2974 (2022).
39. Thirion A, Combes N, Mulliez B et al. BCG-VARS: BallistoCardioGraphy vital algorithms for real-time systems. *Biomed Signal Process Control* **87**, 105526 (2024).
40. Su QS, Zhao YP, Huang YQ et al. Multi-scale attention convolutional neural network for noncontact atrial fibrillation detection using BCG. *Biomed Signal Process Control* **92**, 106041 (2024).
41. Amin MG, Ravisankar A, Guendel AR. RF sensing for continuous monitoring of human activities for home consumer applications. *arXiv - CS - Machine Learning*. https://doi.org/10.1117/12.2519984
42. Kazim JUR, Tahir A, Rains J et al. In-home monitoring using wireless on the walls for future healthcare: real-world demonstration. *Adv Intell Syst* **5**, 2300007 (2023).
43. An YJ, Kim BH, Yun GH et al. Flexible non-constrained rf wrist pulse detection sensor based on array resonators. *IEEE Trans Biomed Circuits Syst* **10**, 300–308 (2016).
44. Liu HH, Hu DJJ, Sun QZ et al. Specialty optical fibers for advanced sensing applications. *Opto-Electron Sci* **2**, 220025 (2023).
45. Zhang L, Zhen YQ, Tong LM. Optical micro/nanofiber enabled tactile sensors and soft actuators: a review. *Opto-Electron Sci* **3**, 240005 (2024).
46. Jiang BQ, Hou YG, Wu JX et al. In-fiber photoelectric device based on graphene-coated tilted fiber grating. *Opto-Electron Sci* **2**, 230012 (2023).
47. Jin HY, Wang ZR, Chen ZL et al. Non-contact sleep atrial fibrillation monitoring using fiber optic sensors. *Proc SPIE* **13639**, 136398V (2025).
48. Jin HY, Wen JF, Chen ZL et al. Multifunctional mattress-type physiological monitoring system with all-fiber structure. In *Proceedings of the 28th International Conference on Optical Fiber Sensors* Tu3.4 (Optica Publishing Group, 2023). http://doi.org/10.1364/OFS.2023.Tu3.4.
49. Shaffer F, Ginsberg JP. An overview of heart rate variability metrics and norms. *Front Public Health* **5**, 258 (2017).
50. Bonnemeier H, Richardt G, Potratz J et al. Circadian profile of cardiac autonomic nervous modulation in healthy subjects: differing effects of aging and gender on heart rate variability. *J Cardiovasc Electrophysiol* **14**, 791–799 (2003).
51. Pfeiffer D, Jurisch D, Neef M et al. Alkohol und Rhythmusstörungen. *Herz* **41**, 498–502 (2016).
52. Wu L, Shi P, Yu HL et al. An optimization study of the ultra-short period for HRV analysis at rest and post-exercise. *J Electrocardiol* **63**, 57–63 (2020).
53. Saiz-Vivo J, Corino VDA, de Melis M et al. Clinical and heart rate variability feature analysis of pre-ablation AF patients leading to recurrence. *J Electrocardiol* **69**, 84 (2021).
54. Egbe AC, Connolly HM, Khan AR et al. Outcomes in adult Fontan patients with atrial tachyarrhythmias. *Am Heart J* **186**, 12–20 (2017).
55. Hanna J, Kyranis S, Alghamry A et al. Coronary artery disease distribution in patients presenting with symptomatic atrial fibrillation. *Heart, Lung Circ* **25**, S38 (2016).
56. Grubb A, Aleong R, Rosenberg MA et al. Development and validation of the Atri-Risk Conduction Index risk score to predict risk of atrial fibrillation after typical atrial flutter ablation. *Heart Rhythm* **21**, 1621–1629 (2024).
57. Castellanos A, Moleiro F, Saoudi N et al. Does complexity theory apply to the conduction ratios occurring during progression of stable atrial flutter with 2: 1 into 4: 1 atrioventricular block. *Am J Cardiol* **75**, 947–949 (1995).
58. Waldo AL. The interrelationship between atrial fibrillation and atrial flutter. *Prog Cardiovasc Dis* **48**, 41–56 (2005).
59. Tanaka K, Fujimura O. Analysis of variable conduction ratios into the atrioventricular node during atrial flutter: multilevel block theory. *HeartRhythm Case Rep* **5**, 274–276 (2019).
60. Li LY, Li YP, Yang LY et al. Continuous and accurate blood pressure monitoring based on wearable optical fiber wristband. *IEEE Sens J* **21**, 3049–3057 (2021).
61. Li LY, Liu YF, Song CY et al. Wearable alignment-free microfiber-based sensor chip for precise vital signs monitoring and cardiovascular assessment. *Adv Fiber Mater* **4**, 475–486 (2022).
62. Li LY, Sheng SF, Liu YF et al. Automatic and continuous blood pressure monitoring via an optical-fiber-sensor-assisted smartwatch. *PhotoniX* **4**, 21 (2023).
63. Still CH, Moore SM, Sattar A. Effects of the intensity of lifestyle exercise on changes in blood pressure. *West J Nurs Res* **43**, 613–621 (2021).
64. Oh DJ, Hong HO, Lee BA. The effects of strenuous exercises on resting heart rate, blood pressure, and maximal oxygen uptake. *J Exerc Rehabil* **12**, 42–46 (2016).

Acknowledgements

We would like to thank the staff and patients of Tongji Hospital, Tongji Medical College, Huazhong University of Science and Technology, for their generous support of our work. We are grateful for financial supports from China National Funds for Distinguished Young Scientists (grant no. 62425505); the National Natural Science Foundation of China (grant no. 623B2034); the Fundamental Research Funds for the Central Universities under Grand YCJJ20241407 and the Fundamental Research Funds for the Central Universities (2024BRA012); Shaanxi Postdoctoral Innovation Talents Support Program Grant Number (2025SQBC014); China Postdoctoral Science Foundation Grant Number 2025M780795

Author contributions

H. Jin constructed the VSMP, completed the signal separation algorithm, and conducted main data analysis and manuscript writing. Z. Chen completed the prototype construction, signal demodulation algorithm, and part of the data analysis work, and participated in part of the manuscript revision work. The initial concept of this work was developed by Pro. Q. Sun and Dr. H. Li, who also established the experimental methodology. Both authors were actively involved in manuscript preparation and iterative revisions. Pro. F. Wang provided guidance on the medical theories related to CA and organized the recruitment and testing of volunteers with CA disease. J. Wen, Z. Wang and K. Zhou completed the hardware circuit design and embedded algorithm for the prototype, as well as the Bluetooth signal transmission component. Dr. W. Hang and Pro. C. Chen provided a lot of valuable feedback during the test of VSMP and played an indispensable role in the selection of CA volunteers and communication with volunteers. L. Li, J. Chen, C. Fan and Z. Yan provided important input for the drafting and revision of the manuscript. K. Shen and J. Wen provided important support in the experimental verification and blood pressure experiments conducted at the HUST-Wuxi Research Institute. All authors reviewed and approved the final manuscript.

Competing interests

The authors declare no competing financial interests.

Supplementary information

Supplementary information for this paper is available at
https://doi.org/10.29026/oea.2026.250334

Open Access This article is licensed under a Creative Commons Attribution 4.0 International License, which permits use, sharing, adaptation, distribution and reproduction in any medium or format, as long as you give appropriate credit to the original author(s) and the source, provide a link to the Creative Commons license, and indicate if changes were made. To view a copy of this license, visit http://creativecommons.org/licenses/by/4.0/
©The Author(s) 2026.
Published by Editorial Office of *Opto-Electronic Advance*, Institute of Optics and Electronics, Chinese Academy of Sciences.

Opto-Electronic Journals Group
www.oejournal.org

Scan for Article PDF